Spatial origin of the neutron-induced background in the JET tangential gamma ray spectrometer

Published by IOP Publishing for Sissa Medialab

Received: *February 27, 2026*
Accepted: *March 11, 2026*
Published: *April 15, 2026*

International Conference on Fusion Reactor Diagnostics: the Burning Plasma Era
Varenna, Italy
1–5 September 2025

Spatial origin of the neutron-induced background in the JET tangential gamma ray spectrometer

S. Colombi,[a,*] **M. Rebai**,[b] **G. Mariano**,[c] **G. Marcer**,[b] **A. Dal Molin**,[b] **D. Rigamonti**,[b] **E. Perelli Cippo**,[b] **M. Nocente**,[a] **S. Fugazza**,[a] **F. Scioscioli**,[a,b] **G. Croci**,[a,b] **M. Tardocchi**[b,a] **and JET contributors**[1]

[a] *Department of Physics, University of Milano-Bicocca, Piazza della Scienza 3, 20126, Milano, Italy*
[b] *ISTP, National Research Council of Italy, Via Roberto Cozzi 53, 20125, Milano, Italy*
[c] *Diagnostic Program, ITER Organization, Saint Paul-lez-Durance, France*

E-mail: s.colombi11@campus.unimib.it

Abstract: The JET tangential gamma ray diagnostic had several key functions, mainly alpha particle detection, runaway electron monitor and recently fusion power estimation. All these measurements are affected by a common background, which can complicate signal detection and whose origin is not yet fully understood. A method to simulate such a background has previously been proposed, however it does not address the spatial origin of the background nor the isotopes responsible for its generation. In this work, we combine simulation tools, including MCNP, with analytical codes to better understand the sources of the background measured with the JET tangential gamma ray diagnostic. The role of the gamma ray flux produced in the tokamak central column is analysed in detail and its correlation with the detected gamma ray background is found.

Keywords: Nuclear instruments and methods for hot plasma diagnostics; Gamma detectors (scintillators, CZT, HPGe, HgI etc); Simulation methods and programs

*Corresponding author.

[1] See the author list of "Overview of T and D-T results in JET with ITER-like wall" by CF Maggi et al. to be published in Nuclear Fusion Special Issue: Overview and Summary Papers from the 29th Fusion Energy Conference (London, U.K., 16–21 October 2023).

https://doi.org/10.1088/1748-0221/21/04/C04034

Contents

1 Introduction

The use of gamma ray spectrometers (GRS) on tokamaks is extensive and mature, with systems that have been deployed for many years and installed on various fusion research devices. Among these, at JET several high-performance instruments based on $LaBr_3$:Ce scintillators have been installed in the last two decades to perform fast ion measurements [1–4], runaway electron studies 5 and, more recently, fusion power [6, 7]. One of these $LaBr_3$ based diagnostic is the tangential gamma ray spectrometer [8], composed of a 19.7 m long line of sight, with a 93 cm lithium hydride neutron attenuator to reduce the direct neutron flux. The detector consists of a $3'' \times 6''$ $LaBr_3$ crystal coupled with a photomultiplier tube, capable to perform spectroscopic measurements of incoming gamma rays, that is essential for distinguish the physics phenomena that produced them. The energy usually ranges between 1 and 20 MeV in the case of fast ion detection and fusion power; for the case of gamma rays emitted from runaway electrons the energy can reach up tens of MeV. When inserted in a neutron environment, such as JET, in addition to signals, a gamma detector also measures gamma rays originated by the interactions of neutrons with all the materials of the environment: the tokamak itself, the walls and every material present in the torus hall. These background events overlap with the events due to signal gamma rays complicating the measurements. The JET spectrum in the DTE2 and DTE3 campaigns has a plateau region extending up to about 8 MeV, see [6], ending with the peaks due to neutron capture on ^{58}Ni (at 8.553 and 8.998 MeV) [9]. Above 9 MeV the spectrum has a sharp drop and the peak of ^{53}Cr at 9.719 MeV.

The study of these neutron induced gammas is usually obtained using Montecarlo codes for neutron and gamma transport, such as MCNP, and detailed models of JET and surrounding structures have been extensively developed since many years [10].[1] In figure 1 a top-down section view of the MCNP model of JET is shown: the line of sight of the tangential gamma spectrometer starts at the port of the tokamak, passes through two collimators, crosses the south concrete wall and then reaches a 93 cm LiH attenuator [11]. The line of sight inside the vessel partially intercepts the central column, while another part intercepts the outer wall, in proximity of the LH antenna.

[1] Model developed by Sean Conroy, JSI institute, A Zohar, R. Villari & Neutronic team ENEA.

2026 JINST 21 C04034

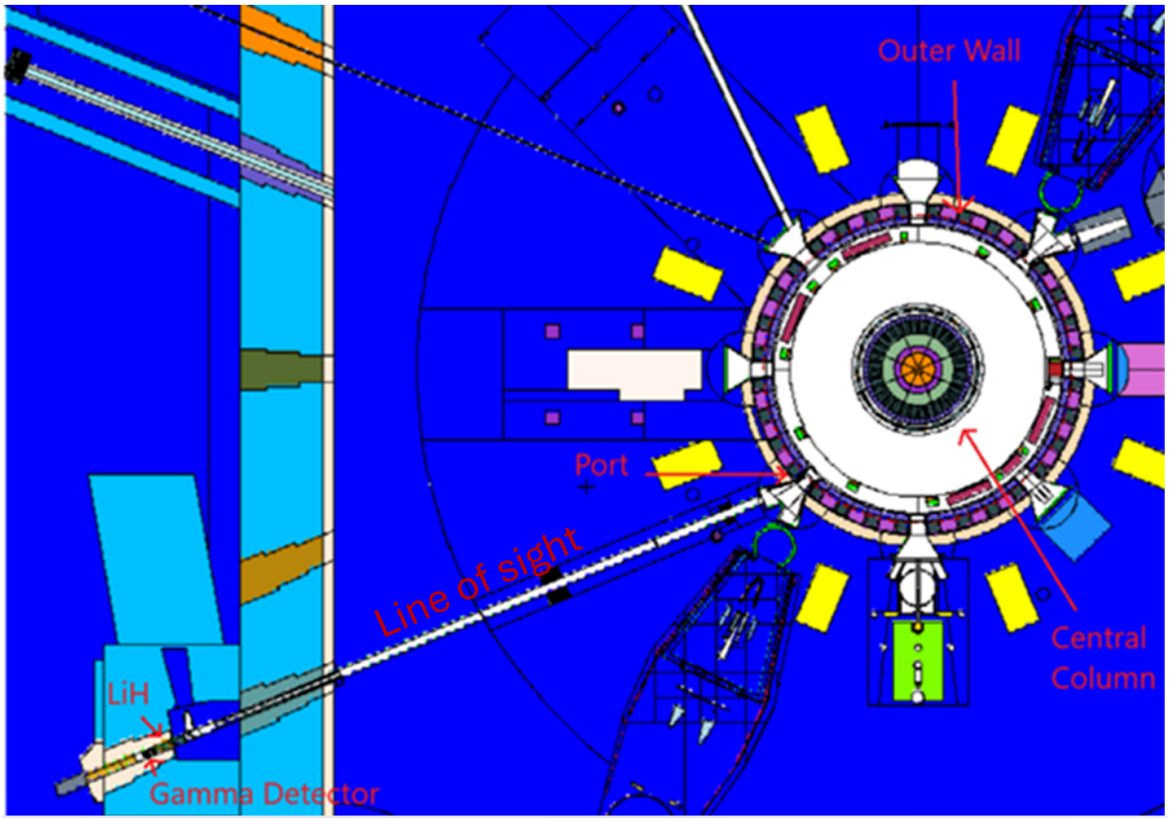

Figure 1. A section of the MCNP model, zoomed on the line of sight of the gamma detector (bottom left).

2 Source of the gamma background

2.1 Spatial origin

There are many possible spatial origins of the neutron induced background that is measured by the detector: the prompt gamma can be generated i) in the neutron attenuator, ii) in the line of sight from the end of the attenuator till the port in the vessel iii) in the central column that is partially intercepted by the line of sight and iv) in the outer wall of the vessel.

The IMP card of MCNP was used to kill all gamma rays passing in a certain cell, to identify which of these give the greatest contribution to the background. To study the effect of the central column, two simulations have been performed: a reference case using the default settings, and a second case in which the importance card of the cell surrounding the central column is modified to suppress all gamma transport while allowing neutrons to propagate unperturbed (IMP:P=0 and IMP:N=1). In both simulations, the tally measures the gamma current reaching the front face of the detector. When the contribution from the central column is removed, the resulting gamma current is nearly an order of magnitude lower than in the default configuration (see figure 2).

The result found shows that neutron induced gammas coming from the central column are the dominant contribution to the gamma flux at the detector, while neutron induced gammas from other sources have a much smaller impact.

The variance reduction technique DXtran has been used, since it is the best tool to model gamma background below 10 MeV, as it simulates well both the neutron scattering in the environment and the transport of neutron induced gammas along a line of sight [12].

2026 JINST 21 C04034

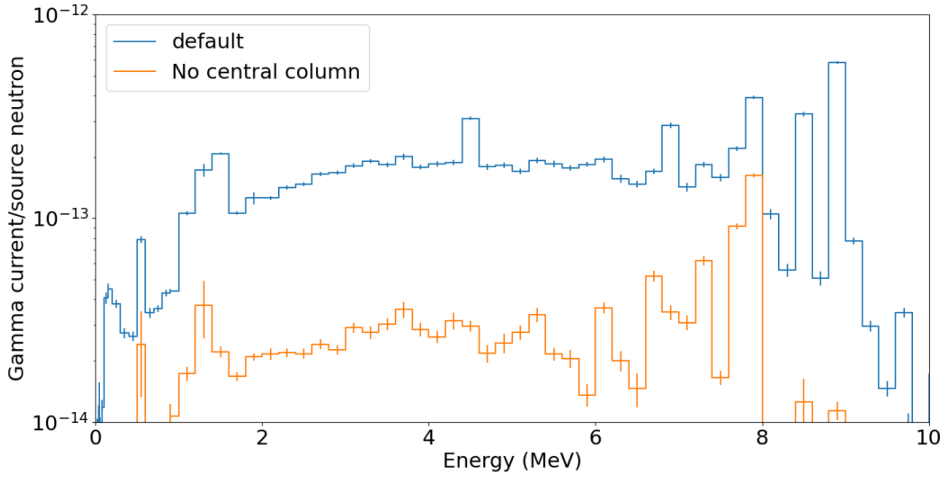

Figure 2. Comparison, in logarithmic scale, between the spectrum of the gamma current on the face of the detector obtained using the default mode (blue line) and the same spectrum using the model without the central column gamma contribution (orange). Results are normalized per source neutron.

2.2 Isotopes contributions

Another aspect that can be investigated using simulations is the identification of the isotopes that contribute most significantly to the background. To this end, the MCNP card PIKMT [13] is used to enable or disable gamma production from neutrons in specific isotopes.

If we enable only the gamma production from chromium and nickel isotopes, the gamma current at the detector surface is quite similar to the default one: that is because chromium and nickel are the main components of Inconel, the main material used in the central column of JET (figure 3). We can conclude that Chromium and Nickel are the isotopes that contribute most to the gamma background, similarly to the conclusion given by Dal Molin et al. [6] where the peaks of ^{58}Ni at 8.533 and 8.998 MeV and of ^{53}Cr at 9.719 MeV have been identified in the measured pulse height spectrum.

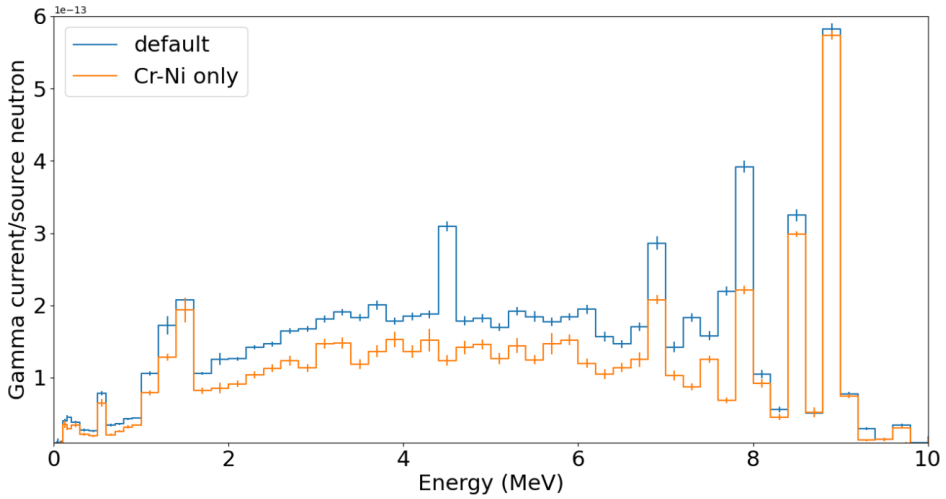

Figure 3. Comparison, in linear scale, between the spectrum of the gamma current on the face of the detector obtained in the default simulation, and in the simulation where the only prompt gamma being produced are the one of Nickel and Chromium, main components of Inconel.

2026 JINST 21 C04034

3 Gamma flux at central column

Given the importance of the gamma flux emitted from the first wall of the central column, further simulations have been performed to characterize the prompt gamma flux in this region.

The simulation was conducted with the full JET model. The flux at the first wall of the central column was measured using a tally imposed on the lateral surface of a cylinder posed around the central column, (radius of 185 cm and height of 10 cm). The tally divides the results in 18 sections according to the angle at which the prompt gamma crosses the tally surface (Card C in MCNP — every 10°).

In particular, the results between 60° and 70°, w.r.t. the normal of the cylinder lateral surface, are of particular interest. This spherical segment includes the angle of inclination of the gamma diagnostic, whose line of sight is positioned 67.5° respect to the radial position.

3.1 Spectral shape and intensity

The energetic spectra of each spherical sector between 0 and 90° doesn't change in shape. Instead, if the intensity (normalized by the area of the corresponding spherical sector), is compared, the radial intensity (from 0 to 10°) of the prompt gamma is more intense than the intensity at a greater angle respect to the normal. In fact, as visible in figure 4, the ratio in the intensity of the spherical sector between 0 to 10° and between 60 and 70° is around 0.5.

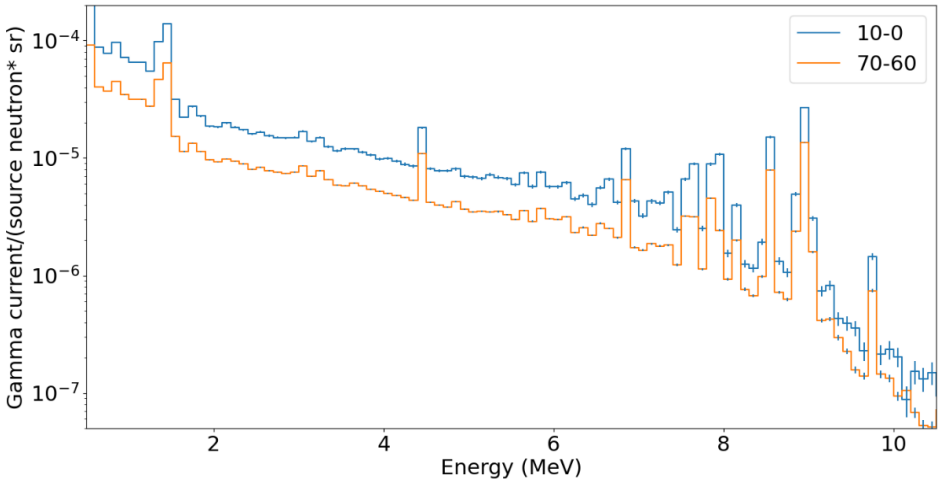

Figure 4. Comparison between the gamma current measured on the central column, for different angles respect to the normal at the surface. Each spectrum has been divided by the respective solid angle.

3.2 Expected detector response

Since most of the background of the gamma detector comes from the central column, the next logical step is to verify whether it is possible, knowing the gamma flux from the central column, to calculate the expected background at the detector using geometrical considerations and a dedicate stand-alone simulation.

The stand-alone simulation takes into account, as shown in figure 5 the materials that gamma rays pass through before reaching the detector, i.e. the LiH attenuator, composed with LiH pellets enclosed in a SS frame, and the response of the detector itself. To calculate this, the attenuator and the detector were extracted from the complete JET MCNP model and simulated in a stand-alone MCNP

2026 JINST 21 C04034

script (figure 5). The gamma ray source used is a perfectly collimated disk source, with a radius equal to the collimator one and with an energy spectrum equal to the one exiting with an angle between 70 and 60 degrees from the central column (figure 4, 70-60 component). The output parameter is therefore a pulse height tally, F8, that is the Detector Response, *DR*.

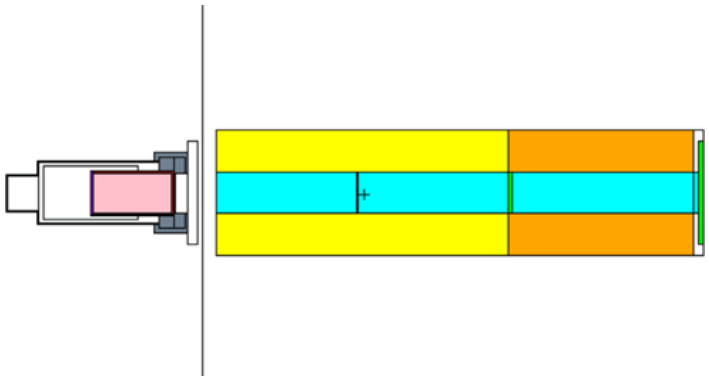

Figure 5. Section view of the MCNP model used to calculate the detector response, showing the gamma detector (pink, on the left), the LiH attenuator (light blue) and stainless steel (light green).

To renormalize the DR spectrum obtained with the stand-alone simulation to the one that has been measured experimentally we have to consider the geometrical parameters that describes the line of sight. In particular, the final detector response is:

$$\text{Final detector response} = N_{\text{yield}} \cdot \frac{A_{\text{detector}}}{A_{\text{sphere}}} \cdot \frac{A_{\text{seen}}}{A_{\text{tally}}} \cdot F_1 \cdot DR$$

Where:

- N_{yield} is the neutron yield for the shots we want to compare with the simulation.
- F_1 is the number of the prompt gammas emitted by the central column with an angle between 60 and 70° respect to the normal to the surface, normalized per source neutron calculated by MCNP.
- A_{tally} is the lateral area of the cylinder added around the central column, on which the tally is defined.
- A_{seen} is the area of the central column intercepted by the line of sight of the gamma diagnostic, calculated with the analytical software Linalytic [14] by specifying the positions of the collimators and the detector.
- A_{detector} is the area of the front face of the gamma detector.
- A_{sphere} is the area of the spherical sector between 60 and 70° with radius R equal to the distance between the central column first wall and the detector, calculated as:

$$\begin{aligned} A_{\text{sphere}} = 2\pi Rh &= 2\pi R^2 \left[(1 - \cos(70°)) - (1 - \cos(60°))\right] \\ &= 2\pi R^2 (\cos(60°) - \cos(70°)) \end{aligned}$$

2026 JINST 21 C04034

If we compare this simulated detector response to the experimental detector one, we find a very good agreement (figure 6). The spectrum has the same shape and intensity as the experimental one: a long plateau until 8 MeV, followed by the peaks of ^{58}Ni and ^{53}Cr and, finally, a sharp decline.

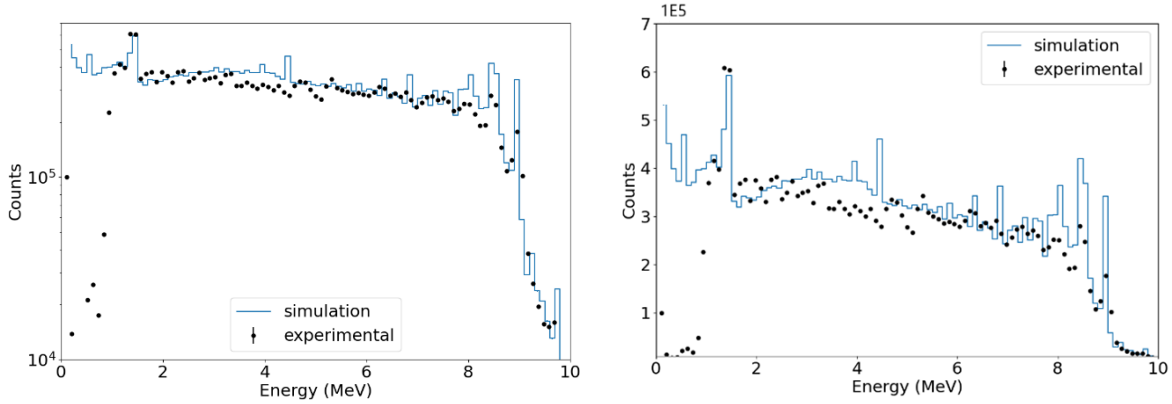

Figure 6. Comparison between the experimental spectrum and the simulated response function, multiplied by the "total" coefficient illustrated in eq. 4, in logarithmic (left) and linear scale (right).

The fact that the simulated detector response to neutron-induced gammas originated in the central column matches the experimental results proves that the background is almost entirely originated in the central column of JET.

Some discrepancies between the simulated and the experimental results can be observed in figure 6: the 4.44 MeV peak of carbon is missing in the experimental spectrum, and the peaks of ^{58}Ni at 8.533 and 8.998 MeV, have a different height with respect to the one measured experimentally. For a more accurate model, a detailed MCNP transport simulation has to be used [12].

4 Conclusions and considerations for future gamma diagnostics

The analysis presented in this work demonstrates that the dominant contribution to the gamma-ray background measured by the JET tangential gamma spectrometer originates from neutron-induced gamma emission in the central column. Through a combination of stand-alone MCNP simulations, cell importance filtering and isotope-specific gamma-production studies, it was shown that suppressing gamma transport from the central column reduces the detected flux by nearly an order of magnitude, clearly identifying this region as the primary source of background. The isotopic analysis further confirms that chromium and nickel, key constituents of the Inconel structure, are responsible for most of the observed spectral features, in agreement with experimental observations.

By characterizing the angular distribution and spectral shape of the prompt gamma flux emitted from the central column and by propagating this flux through a dedicated stand-alone simulation of the LiH attenuator and detector, it was possible to reconstruct the expected detector response with a good fidelity. The simulated spectrum reproduces both the intensity and the shape observed experimentally, validating the conclusion that the central column dominates the background. Some discrepancies remain, such as the absence of the 4.44 MeV carbon peak and differences in the relative heights of the nickel lines, but these can still be addressed through a full MCNP transport calculation.

2026 JINST 21 C04034

The approach developed here provides a fast and flexible tool for predicting gamma-ray backgrounds in other tokamaks, enabling rapid assessments of expected background spectral features and count rates based on geometry and material composition. This capability is particularly valuable for the design and optimization of gamma-ray diagnostics in next-generation fusion devices, such as ITER, where accurate background estimation is essential. In particular, given the importance of the central column contribution to the background, in future machines the diagnostic should avoid direct visibility of it. For example, tangential gamma-ray spectrometers whose line of sight extends to the other side of the outer wall and continues onto another tangential line of sight would significantly reduce background level, enhancing the quality and sensitivity of gamma-ray measurements.

Acknowledgments

This work was done as a part of a PhD supported by Eni in the framework of the Italian D.M. 117/2023. This work has been carried out within the framework of the EUROfusion Consortium, funded by the European Union via the Euratom Research and Training Programme (Grant Agreement No. 101052200 — EUROfusion). Views and opinions expressed are however those of the author(s) only and do not necessarily reflect those of the European Union or the European Commission. Neither the European Union nor the European Commission can be held responsible for them.

References

[1] M. Nocente et al., *MeV range particle physics studies in tokamak plasmas using gamma-ray spectroscopy*, *Plasma Phys. Control. Fusion* **62** (2019) 014015.

[2] V.G. Kiptily et al., *Recent progress in fast ion studies on JET*, *Nucl. Fusion* **49** (2009) 065030.

[3] M. Nocente et al., *Generation and observation of fast deuterium ions and fusion-born alpha particles in JET D-^{3}He plasmas with the 3-ion radio-frequency heating scenario*, *Nucl. Fusion* **60** (2020) 124006.

[4] M. Iliasova et al., *Gamma-Ray Measurements in D ^{3}He Fusion Plasma Experiments on JET*, *Nucl. Instrum. Meth. A* **1031** (2022) 166586.

[5] A. Dal Molin et al., *A new hard x-ray spectrometer for runaway electron measurements in tokamaks*, *Meas. Sci. Technol.* **34** (2023) 085501.

[6] A. Dal Molin et al., *Measurement of the Gamma-Ray-to-Neutron Branching Ratio for the Deuterium-Tritium Reaction in Magnetic Confinement Fusion Plasmas*, *Phys. Rev. Lett.* **133** (2024) 055102.

[7] M. Rebai et al., *First Direct Measurement of the Spectrum Emitted by the ^{3}H (^{2}H, γ) ^{5}He Reaction and Assessment of the Relative Yield γ_1 to γ_0*, *Phys. Rev. C* **110** (2024) 014625.

[8] M. Nocente et al., *A new tangential gamma-ray spectrometer for fast ion measurements in deuterium and deuterium-tritium plasmas of the Joint European Torus*, *Rev. Sci. Instrum.* **92** (2021) 043537.

[9] B.B. Kinsey and G.A. Bartholomew, *Neutron Capture γ-Rays from Titanium, Chromium, Iron, Nickel, and Zinc*, *Phys. Rev.* **89** (1953) 375.

[10] A. Žohar et al., *Validation of realistic Monte Carlo plasma gamma-ray source on JET discharges*, *Nucl. Fusion* **62** (2022) 066004.

[11] D. Rigamonti et al., *Role of neutron attenuators for gamma-ray measurements in deuterium-tritium magnetic confinement plasmas*, *Rev. Sci. Instrum.* **93** (2022) 093515.

2026 JINST 21 C04034

[12] S. Colombi et al., *MCNP-based characterization of the High-Energy Background in gamma ray spectrometers for fusion power measurements in DT plasmas*, submitted to *IEEE, special issue — selected papers from SOFE 2025*.

[13] J. Kulesza et al., *MCNP® Code Version 6.3.0 Theory & User Manual*, LA-UR-22-30006 (2022).

[14] G. Marcer et al., *Development of a measuring technique based on JET second D-T campaign (DTE2) experience for assessing fusion power at ITER during D-T operation using the radial gamma-ray spectrometer*, *Rev. Sci. Instrum.* **95** (2024) 083515.

2026 JINST 21 C04034